

A SIMPLE ANALYSIS OF THE INFLUENCE OF STRAIN AND CURVATURE ON LAMINAR PREMIXED FLAMES

T. TAKENO⁺* and Ken BRAY[#]

⁺*Professor Emeritus, Graduate School of Engineering*

(Received January 18, 2002)

Abstract

The aim of this work is to describe the influence of nonuniform flow on laminar flames. A simple steady flow analysis is presented in which gas density and molecular transport coefficients are assumed constant and a global reaction rate expression is employed in the high activation energy asymptotic limit. Considerable further simplification is achieved by a priori specification of a function related to the mass flow rate normal to the flame. The analysis allows the influence of flame curvature and strain on the mass burning rate to be clearly identified. It is shown that, except in the weak stretch limit, the relationship between mass burning rate and flame stretch is dependent on flame geometry. Conversely the mass burning rate is uniquely related to the temperature gradient at the reaction surface irrespective of flame geometry.

Keywords: flame theory, effects of nonuniform flow, asymptotic analysis

1. Introduction

The propagation of laminar flames in nonuniform flows has been studied for many years both because of the intrinsic importance of the subject and in view of applications to laminar flamelet models of turbulent combustion (Peters 1986, Bray and Peters 1994). Reviews of the extensive literature on laminar flames may be found in Buckmaster and Ludford (1982), Williams (1985), Clavin (1985), Law (1988) and Linan and Williams (1993).

*Present address: Department of Department of Mechanical Engineering, Meijo University, Tenpaku-ku, Nagoya 468-8502, Japan

#Present address: Engineering Department, Cambridge University, Trumpington Street, Cambridge, CB2 1PZ, England

Activation energy asymptotic analysis (AEA: Buckmaster and Ludford 1982, Williams 1985, Calvin 1985, Linan and Williams 1993, Matalon and Matkowsky 1982) is based on the observation that the activation energy of a global combustion reaction is typically large in comparison with thermal energy. It has proved to be both a powerful analytical tool and an aid to understanding of the interactions between flame propagation and nonuniform flow. In AEA the flame consists of a relatively thick preheat zone, in which convective and diffusive processes are in balance, followed by a thin layer where heat release occurs, and where a diffusive – reactive balance exists. To match the solutions for these two zones for adiabatic flames, the rate of heat release in the thin reaction layer is equated to the rate at which heat is lost by conduction to the preheat zone. Consequently the heat release rate is uniquely related to the temperature gradient at the hot side of the preheat zone. This perspective remains valid when time-dependent curvature and strain are considered (Joulin 1994).

A more detailed analysis of the structure of a methane-air flame (Peters and Williams 1987) makes use of a three-step reduced reaction mechanism. The thin reaction layer of AEA is replaced by a fuel consumption layer followed by an oxidation layer, but both layers are thin in comparison with the preheat zone. As before the temperature gradient at the edge of the preheat zone is related to the heat release rate due to combustion.

Application of AEA to weakly disturbed flow fields with large characteristic length scales in comparison with the thickness of the preheat zone (Sivashinsky 1977, Clavin and Williams 1982, Clavin and Joulin 1983, Clavin 1985), forms the basis of many studies of flame dynamics. An important result of these perturbation analyses is to predict a linear relationship between the laminar flame speed S_d and the flame stretch

$$\frac{1}{\tau_s} = \frac{1}{\Delta A} \frac{d\Delta A}{dt} = (\nabla_{\mathbf{t}} \cdot \mathbf{v})_{x^*} - S_d / R^*$$

(Chung and Law 1984, Candel and Poinso 1990) where ΔA is the area of an element of flame surface, $\nabla_{\mathbf{t}}$ is the component of the ∇ operator which is tangential to the flame and $1/R^* = \nabla_{\mathbf{t}} \cdot \mathbf{n}$ is the flame curvature at $x = x^*$, where x^* is the position of the thin reaction zone, \mathbf{n} being a unit vector directed towards reaction products. This linear relationship between S_d and the burning velocity S_u of the unstretched flame is predicted to be

$$\frac{S_d}{S_u} = 1 - \mu K$$

where $K = \frac{\delta}{S_u} \frac{1}{\Delta A} \frac{d}{dt} \Delta A$ is a dimensionless flame stretch factor and δ is the flame thickness. The Markstein number μ is a measure of flame sensitivity to stretch and can be expressed as a function of Lewis number and other properties (Clavin 1985). According to this small perturbation analysis K is the single parameter, which describes the influence of both strain and curvature on flame propagation in a given mixture so long as $K \ll 1$. If the flame is stationary, as is assumed here, the velocity vector \mathbf{v} can be decomposed into a normal component $S_d \mathbf{n}$ and a tangential component \mathbf{v}_t . The curvature term in the equation defining the flame stretch then cancels with

$$\nabla_{\mathbf{t}} \cdot (S_d \mathbf{n})$$

and the stretch relationship reduces (Poinso *et al.* 1992) to

$$\frac{1}{\tau_s} = \frac{1}{\Delta A} \frac{d\Delta A}{dt} = (\nabla_{\mathbf{t}} \cdot \mathbf{v})_{x^*} - S_d / R^* = (\nabla_{\mathbf{t}} \cdot \mathbf{v}_t)_{x^*}$$

where S_d is the local burning velocity at $x = x^*$, and R^* is the curvature of the reaction sheet.

Analysis by AEA of nonlinear problems in which K is not small is usually confined to

particular flame geometries such as a counterflow flame (Libby and Williams 1982, 1983, 1984, 1988, Libby *et al.* 1983b) or a tubular or cylindrical flame (Takeno *et al.* 1986a, 1986b, Libby *et al.* 1989). Sudden extinction is predicted in some situations but not in others so the K can no longer be regarded as the single parameter to describe the influence of flow nonuniformity. These solutions depend on geometry as well as stretch as do predictions from the integral analysis of Chung and Law (1988, 1989). Similar behavior may be found in numerical solutions (see for example Peters and Rogg 1993, Bradley *et al.* 1996).

For turbulent combustion Poinso *et al.* (1991) identify an extended range of flamelet burning conditions under which the turbulence intensity is insufficient to cause local extinction. However, in part of this range, small turbulent eddies can influence the preheat zone structure and experiments (Chen *et al.* 1996, Buschmann *et al.* 1996, O'Young and Bilger, 1997) indicate a thickening of the preheat zone. A laminar flamelet model of turbulent combustion must describe the effects of the local flow field on the local mass burning rate of the flamelet, and must do so in terms of predictable quantities. Direct numerical simulations of turbulent combustion (Poinso *et al.* 1995) show that this mass burning rate cannot be well correlated with tangential strain, curvature or stretch.

The present paper describes a simple theoretical model of a laminar flame in a nonuniform flow field. Its aim is to derive algebraic expressions for the flame structure and mass burning rate in a sufficiently simple form so that the influence of strain and curvature can be identified and understood. In pursuit of these aims the following drastic simplifying assumptions are introduced. The flow is taken to be two-dimensional and steady and the problem is reduced to one dimension by a priori specification of the variation with distance x normal to the flame of a mass flow function $M(x)$. Density and molecular diffusivities are assumed constant. A global chemical reaction is specified and a conventional AEA analysis is performed on the assumption that conditions leading to extinction are avoided. The resulting model is considered to be appropriate for a qualitative description of the effects of nonuniform flow on the flame.

The development of the model is described in Section 2. Simple algebraic expressions are derived for the temperature and composition distributions as well as the mass burning rate which is shown to be uniquely related to the temperature gradient at the hot edge of the preheat zone. In Section 3 the analysis is applied to flows in which the mass flow function $M(x)$ is specified to be constant allowing the effects of flame curvature to be studied in the absence of strain. Examples of flows in which $M(x)$ is not constant are analyzed in Section 4 and qualitative differences between the behavior of planar and cylindrical strained flames are identified and explained. Finally in Section 5 these results are expressed in terms of the stretch parameter K . It is clearly demonstrated that conventional measure of flame strength depend not only on K and the Lewis number but also on the flow geometry as expressed in the mass flow function $M(x)$. However, established results are recovered in the limit of weak stretch where K and the Lewis number do describe all effects of strain and curvature.

We conclude that in general the effects of strain and curvature are dependent on geometry. On the other hand the relationship between the mass burning rate and the temperature gradient at the hot side of the preheat zone is robust and independent of flame geometry.

2. Analytical Model

The analysis is based on the assumption that the flame consists of a thick diffusion layer, or preheat zone, and a thin reaction zone in which the reaction goes to completion. The flame and the flow are steady and the gas density is assumed to be constant and unaffected by the combustion

reaction. We assume that the flame can be described in terms of similarity solutions, and that the flame is one-dimensional, either plane ($j = 0$) or cylindrical ($j = 1$), while the flow is two-dimensional (Takeno *et al.* 1986a, 1986b, 1993, Nishioka *et al.* 1988, 1991, 1994). Then the flame structure can be described in terms of a single space coordinate x normal to the flame. The temperature, T , the mass fraction Y_i of species i and the velocity component, u , normal to the flame depend only on x , so $T = T(x)$, $Y_i = Y_i(x)$, $u = u(x)$. The pressure is assumed to be constant. In the present analysis we are concerned only with possible nonuniformities of the mass flux normal to the flame. The flow field is a function of x and y , the coordinate normal to x , and we do not solve the momentum equation. Instead, we assume that the mass flux m normal to the flame is given as a function of x . In some cases a hypothetical mass source or sink must be placed at $x = x_{min}$ to produce the given flow field. The velocity component v parallel to the flame is determined so as to satisfy mass conservation. The Soret and Dufort effects, as well as pressure diffusion, are neglected. The specific heat c_p and thermal conductivity λ of the mixture are constant. The diffusion velocity vector V_i is given by the simple Fick's law expression.

$$Y_i V_i = -D \nabla Y_i \quad (1)$$

where the diffusion coefficient D is assumed to have the same constant value for all species i . The mixture undergoes an overall one-step reaction described by

$$v_F F + v_{ox} O + v_I I = v_P P + v_I I \quad (2)$$

where F , O and I refer to fuel, oxygen and inert, respectively. The reaction order is unity with respect to both fuel and oxygen.

The governing equations are the species conservation equations and the energy equation. In general form, they are

$$\nabla \cdot [\rho Y_i (\mathbf{v} + \mathbf{V}_i)] = w_i \quad (3)$$

$$\nabla \cdot [\rho \sum_i h_i Y_i (\mathbf{v} + \mathbf{V}_i) - \lambda \nabla T] = 0 \quad (4)$$

where ρ , \mathbf{v} , w_i and h_i are the density, velocity vector, mass production rate and specific enthalpy of species i , respectively. Now, the mass flux fraction for species i is introduced by

$$\varepsilon_i = \rho Y_i (u + V_i) / m, \quad (5)$$

where $m = \rho u$, and V_i is the diffusion velocity of species i in the x direction. In order to study effects of curvature, we also introduce a quantity M related to the total mass flow and defined as

$$M = x^j m = x^j \rho u. \quad (6)$$

Note that ε_i , m and M are all assumed to be functions of x alone, and that m and M are positive or negative, depending on whether the flow is in the positive or negative x direction. In view of the above assumptions, Equation (3) reduces to

$$\frac{1}{x^j} \frac{d}{dx} (M \varepsilon_i) + \rho Y_i \frac{\partial v}{\partial y} = w_i \quad (7)$$

Summation over all i gives the continuity relation

$$\rho \frac{\partial y}{\partial y} = -\frac{1}{x^j} \frac{dM}{dx} \quad (8)$$

and use of this in Equation (7) gives the species conservation equations in the following form

$$d(M\varepsilon_i) - Y_i dM = w_i x^j dx \quad (9)$$

Similar manipulation reduces the energy Equation (4) to

$$d[M\{c_p(T - T^o) - L_e \frac{\rho D x^j}{M} \frac{d}{dx} (c_p T)\}] - c_p(T - T^o) dM = -\sum_i h_i^o w_i x^j dx \quad (10)$$

where T^o is a standard reference temperature, and the Lewis number L_e is given by $L_e = \lambda / (\rho c_p D) = \sigma / D$, where σ is the thermal diffusivity. In the derivation use has been made of the following ideal gas relation

$$h = \sum_i Y_i h_i = \sum_i Y_i h_i^o + c_p(T - T^o) \quad (11)$$

where h_i^o is the standard heat of formation of species i . Now, Equations (9) and (10) are the fundamental equations of the present analysis.

Nondimensional System

A non-dimensional space coordinate ξ is defined as

$$\xi = \int_{x_{\min}}^x \frac{|M|}{\rho D x^j} dx = \int_{x_{\min}}^x \frac{|m|}{\rho D} dx \quad (12)$$

Boundary conditions will be specified at $x = x_{\min}$ where $\xi = 0$. The mass flux fraction for species i is

$$\varepsilon_i = Y_i \pm \frac{dY_i}{d\xi} \quad (M \gtrless 0) \quad (13)$$

In the species conservation Equation (9) we take $i = F$ for fuel. The mass production rate is given by

$$w_F = -\bar{B} Y_F Y_{Ox} \exp(-E_n / \theta) \quad (14)$$

where the nondimensional temperature is defined by $\theta = T/T^o$, and the frequency factor, nondimensional activation energy and heat release are given by

$$\bar{B} = \frac{\nu_F B T^{\alpha_1} \rho^2}{W_{ox}}, E_n = \frac{E}{R^o T^o}, q = \frac{\nu_F W_F h_F^o + \nu_{ox} W_{ox} h_{ox}^o - \nu_p W_p h_p^o}{\nu_F W_F c_p T^o} \quad (15)$$

where B and α_j are constants and R^o and W_i are the universal gas constant and the molecular weight of species i . The fundamental Equations (9) and (10) can be given in terms of these quantities as

$$M dY_F \pm d(M \frac{dY_F}{d\xi}) = -\bar{B} Y_F Y_{ox} \exp(-E_n / \theta) x^j dx \quad (M \gtrless 0) \quad (16)$$

$$Md\theta \pm L_e d(M \frac{d\theta}{d\xi}) = -q\bar{B} Y_F Y_{ox} \exp(-E_n/\theta) x^j dx \quad (M \gtrless 0) \quad (17)$$

where it is convenient to express the right hand sides in terms of x rather than ξ .

The mass flow function $M(x)$ has an important role in this formulation. In the present work it is assumed that $M(x)$ can be specified a priori where the corresponding velocity field is a solution of the Navier Stokes equation. Problems for which $M = \text{constant}$ are analyzed in Section 3 and cases where M is allowed to vary are treated in Section 4.

If $M = \text{constant}$ the flow is uniform, one-dimensional and normal to the flame so $v = 0$. With $j = 0$ the flame is planar. It is stabilized by a line sink of combustion products if $M < 0$, or by a line source of reactants if $M > 0$. When $j = 1$ the flame is cylindrical. If $M < 0$ reactants flow radially inwards into this flame and combustion products are removed at a sink which is placed at the center of the flame. On the other hand, with $M > 0$, unburned reactants are supplied from a central source and flow radially outwards into the flame.

The analysis of flames for which $M = \text{constant}$ can readily be extended to cases where the density ρ is allowed to vary due to heat release. The most important conclusion to emerge is that our description of the qualitative relationship between flame temperature, the reaction rate and processes in the preheat zone is unaffected by changes in density.

Flames stabilized in nonuniform flows ($M \neq \text{constant}$) are of particular interest since they are subject to flame stretch effects due to velocity gradients in the plane of the flame sheet. In these geometries the mass flux of unburned mixture must decrease as the flame is approached from the unburned gas side, otherwise the flame will flash back and we cannot have steady flow. In Section 4 we will study these flames separately for cases where $M < 0$ and $M > 0$. Simple functional forms are chosen for the variation of M with location in the flame and analytical solutions are obtained.

If $M < 0$ the assumption is made that the mass flux m varies linearly with x . Then the case with $j = 0$ corresponds to the familiar twin flame problem (Libby and Williams 1984) in which the flame is planar and the strained flow of combustion products approaches a stagnation point at $x = 0$. With $j = 1$ the geometry is that of a cylindrical or tubular flame (Buckmaster 1979, Libby *et al.* 1989, Takeno *et al.* 1994). Reactants flow radially inwards through the flame and combustion products flow out along the axis of the flame cylinder. Situations where $M > 0$ are illustrated for cases where M is assumed to be inversely proportional to x . For $j = 0$ the solution describes a planar flame in a strained flow whereas with $j = 1$ it represents an axisymmetric tubular flame (Takeno *et al.* 1994, Zhu *et al.* 1995a, 1995b) in which the unburned mixture is injected outwards from a line source on the axis.

Asymptotic Analysis

The analysis will be carried out for the case of a lean mixture, in circumstances where $1 - \phi = O(1) > 0$, where ϕ is the equivalence ratio defined by

$$\phi = \frac{v_{ox} W_{ox} Y_{F,o}}{v_F W_F Y_{ox,o}} \quad (18)$$

Here subscript o indicates the value in an unburned gas mixture. The extension of the analysis to a rich and stoichiometric mixtures is self-evident. The approach follows that of a previous study (Takeno *et al.* 1986b). It is assumed that Le is not necessarily unity but is an order of unity quantity. The Zeldovich number defined by $\beta = E_n/\theta^{*2}$ is large enough to justify the assumption of a thin reaction zone which is referred to as the reaction surface or reaction sheet. Superscript * indicates a value at this reaction sheet so θ^* is the temperature at the reaction sheet, which will

also be referred to as the flame temperature. Solutions are sought (Takeno *et al.* 1986b) by expanding dependent variables in powers of $1/\beta$.

Outer Solutions

In the present analysis only zero'th order outer solutions are required. They determine the structure of the preheat zone and can be obtained (Takeno *et al.* 1986b) by solving the fundamental equations with no reactive terms. The resulting equations are linear and can be solved to give general solutions in an integral form. In the following we present these solutions separately for cases when $M < 0$ and $M > 0$.

Solutions for $M < 0$

Figure 1 shows schematically the temperature and fuel concentration distributions in this case in which the unburned gas, with the dimensionless temperature θ_o and fuel mass fraction $Y_{F,o}$, flows from right to left and the reaction sheet is located at $\xi = \xi^*$. The solutions for the burned gas are trivial and are simply given by

$$0 < \xi < \xi^* : Y_F = 0, \theta = \theta^*. \quad (19)$$

The boundary conditions for the preheat zone are

$$\xi = \xi^* : Y_F = 0, \theta = \theta^*, \quad \xi = \infty : Y_F = Y_{F,o}, \theta = \theta_o. \quad (20)$$

and the solutions satisfying these conditions are

$$Y_F = Y_{F,o} \int_{\xi^*}^{\xi} \frac{e^{-\xi}}{M} d\xi / \int_{\xi^*}^{\infty} \frac{e^{-\xi}}{M} d\xi \quad (21)$$

$$\theta^* - \theta = (\theta^* - \theta_o) \int_{\xi^*}^{\xi} \frac{e^{-\xi/L_e}}{M} d\xi / \int_{\xi^*}^{\infty} \frac{e^{-\xi/L_e}}{M} d\xi \quad (22)$$

Then the concentration and temperature gradients at the reaction sheet are given by

$$\left(\frac{dY_F}{d\xi} \right)^* = Y_{F,o} e^{-\xi^*} / M^* \int_{\xi^*}^{\infty} \frac{e^{-\xi}}{M} d\xi > 0 \quad (23)$$

$$\left(\frac{d\theta}{d\xi} \right)^* = -(\theta^* - \theta_o) e^{-\xi^*/L_e} / M^* \int_{\xi^*}^{\infty} \frac{e^{-\xi/L_e}}{M} d\xi < 0 \quad (24)$$

Solutions for $M > 0$

The temperature and concentration distributions for this case are shown schematically in Figure 2. Here the flow is from left to right. Combustible mixture is supplied at $\xi = 0$ with dimensionless temperature θ_o and fuel concentration $Y_{F,o}$ and the reaction sheet is again located at ξ^* . The solutions for the burned gas are

$$\xi > \xi^* : Y_F = 0, \theta = \theta^*. \quad (25)$$

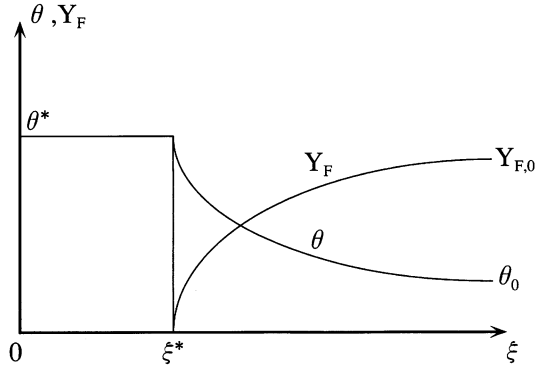


Fig. 1 Schematic representation of temperature and fuel concentration distributions for $M < 0$. The flow is from right to left.

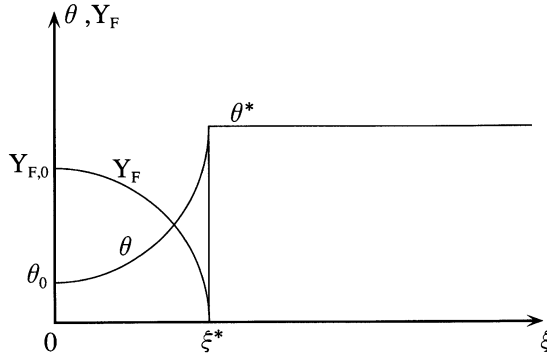


Fig. 2 Schematic representation of temperature and fuel concentration distributions for $M > 0$. The flow is from left to right.

and the boundary conditions for the preheat zone are given by

$$\xi = 0 : Y_F = Y_{F,o}, \theta = \theta_o, \xi = \xi^* : Y_F = 0, \theta = \theta^*. \quad (26)$$

The solutions that satisfy these conditions are

$$Y_F = Y_{F,o} \int_{\xi}^{\xi^*} \frac{e^{\xi}}{M} d\xi / \int_0^{\xi^*} \frac{e^{\xi}}{M} d\xi \quad (27)$$

$$\theta^* - \theta = (\theta^* - \theta_o) \int_{\xi}^{\xi^*} \frac{e^{\xi/L_e}}{M} d\xi / \int_0^{\xi^*} \frac{e^{\xi/L_e}}{M} d\xi \quad (28)$$

Then the concentration and temperature gradients at the reaction sheet are given by

$$\left(\frac{dY_F}{d\xi}\right)^* = -Y_{F,o} e^{\xi/L_e} / M^* \int_0^{\xi^*} \frac{e^{\xi}}{M} d\xi < 0 \quad (29)$$

$$\left(\frac{d\theta}{d\xi}\right)^* = (\theta^* - \theta_o) e^{\xi/L_e} / M^* \int_0^{\xi^*} \frac{e^{\xi/L_e}}{M} d\xi > 0 \quad (30)$$

Inner Solutions

To investigate the structure of the thin reaction zone, or reaction sheet, we introduce an extended space coordinate defined by $\eta = \beta(\xi - \xi^*)$ and expand Y_F and θ as

$$Y_F(\eta) = \frac{1}{\beta} Y_1(\eta) + O\left(\frac{1}{\beta^2}\right) \quad \theta(\eta) = \theta^* - \frac{1}{\beta} \theta_1(\eta) + O\left(\frac{1}{\beta^2}\right) \quad (31)$$

Because the reaction zone is thin a factor on the right hand sides of Equations (16) and (17) can be rewritten as

$$\frac{\bar{B}x^j dx}{|M^*|} = \frac{\bar{B}\rho D}{\beta m^{*2}} d\eta \quad (32)$$

where m^* is the local mass flux at the reaction sheet. Substitution of these relations into Equations (16) and (17), and neglect of higher order terms of $O(1/\beta)$, leads to a balance between diffusion and reaction in the form

$$d\left(\frac{dY_1}{d\eta}\right) = \Lambda^* Y_1 e^{-\theta_1} d\eta \quad (33)$$

$$d\left(\frac{d\theta_1}{d\eta}\right) = \frac{q}{L_e} \Lambda^* Y_1 e^{-\theta_1} d\eta \quad (34)$$

where Λ^* is given by

$$\Lambda^* = \frac{\bar{B} \lambda Y_{ox,o} (1 - \phi)}{L_e c_p \beta^2 e^{E_n/\theta^*} m^{*2}} \quad (35)$$

When the equations are solved under the appropriate boundary conditions, we have the following solutions.

$$Y_1 = \frac{L_e}{q} \theta_1 \quad (36)$$

$$\left(\frac{d\theta_1}{d\eta}\right)^2 = 2\Lambda^* [1 - e^{-\theta_1} (1 + \theta_1)] \quad (37)$$

The solutions for the temperature gradient at upstream ($M > 0$) or downstream ($M < 0$) infinity are

$$\left(\frac{d\theta_1}{d\eta}\right)_{\eta \rightarrow \pm\infty} = \pm \sqrt{2\Lambda^*} \quad (M \lesseqgtr 0) \quad (38)$$

This implies that the temperature gradient at the reaction sheet of the outer solutions must be set equal to

$$\left(\frac{d\theta}{d\xi}\right)^* = \pm \sqrt{2\Lambda^*} \quad (M \geq 0) \quad (39)$$

allowing the inner and outer solutions to be matched. The above expression can be rewritten in the following form

$$\left(\frac{d\theta}{d\xi}\right)^* = \pm \frac{m_o r}{|m^*|} \frac{(\theta_a - \theta_o)}{L_e} \quad (M \geq 0) \quad (40)$$

where m_o and r are defined by

$$m_o = \left[\frac{2L_e \lambda v_F \rho^2 B T^{\alpha_1} Y_{ox,o} (1 - \phi) \theta_a^4}{c_p W_{ox} E_n^2 (\theta_a - \theta_o)^2 e^{E_n/\theta_a}} \right]^{1/2} \quad (41)$$

$$r = \left(\frac{\theta^*}{\theta_a}\right)^2 \exp\left[\frac{E_n}{2} \left(\frac{1}{\theta_a} - \frac{1}{\theta^*}\right)\right] \quad (42)$$

where θ_a is the adiabatic flame temperature defined by $\theta_a = \theta_o + qY_{F,o}$. As will be shown later, m_o represents the mass burning velocity of the normal adiabatic flame, while r represents the effect on the fuel consumption rate of a deviation of the flame temperature from the adiabatic flame temperature.

Matching Conditions

The first matching condition at the reaction sheet is provided by the conservation of enthalpy through it. This condition can be obtained by integrating Equations (16) and (17) through the reaction sheet as

$$\left[\frac{d\theta}{d\xi}\right]_+^+ = -\frac{q}{L_e} \left[\frac{dY_F}{d\xi}\right]_-^+ \quad (43)$$

Substitution of the outer solutions (23), (24), (29) and (30), into Equation (43) yields equations to relate the flame temperature θ^* to the reaction sheet position ξ^* . The results are

$$s = \frac{\theta^* - \theta_o}{\theta_a - \theta_o} = \frac{e^{-\xi^*/L_e} \int_{\xi^*}^{\infty} \frac{e^{-\xi/L_e}}{M} d\xi}{L_e e^{-\xi^*/L_e} \int_{\xi^*}^{\infty} \frac{e^{-\xi}}{M} d\xi} \quad (44)$$

for $M < 0$ and

$$s = \frac{\theta^* - \theta_o}{\theta_a - \theta_o} = \frac{e^{\xi^*/L_e} \int_0^{\xi^*} \frac{e^{\xi/L_e}}{M} d\xi}{L_e e^{\xi^*/L_e} \int_0^{\xi^*} \frac{e^{\xi}}{M} d\xi} \quad (45)$$

for $M > 0$. In these equations, s represents the relative deviation of the flame temperature θ^* from the adiabatic flame temperature θ_a . These equations reveal that the dependence of θ^* on ξ^* is independent of j and is the same for the plane and cylindrical flames provided that M is identical when expressed as a function of ξ . They also show that deviation of the flame temperature from adiabatic occurs only when $Le \neq 1$, that is when there is an imbalance between heat and mass transport. On the contrary, the flame temperature is always equal to the adiabatic flame temperature for unity Lewis number.

The second matching condition is obtained by substituting $(d\theta^*/d\xi)^*$ from the outer solutions (24) and (30) into Equation (40). The results may be written

$$\frac{m_o}{|m^*|} = \frac{sL_e e^{-\xi^*/L_e}}{rM^* \int_{\xi^*}^{\infty} \frac{e^{-\xi^*/L_e}}{M} d\xi} = \frac{L_e}{R} \frac{e^{-\xi^*/L_e}}{M^* \int_{\xi^*}^{\infty} \frac{e^{-\xi^*/L_e}}{M} d\xi} \quad (46)$$

for $M < 0$ and

$$\frac{m_o}{|m^*|} = \frac{sL_e e^{\xi^*/L_e}}{rM^* \int_0^{\xi^*} \frac{e^{\xi^*/L_e}}{M} d\xi} = \frac{L_e}{R} \frac{e^{\xi^*/L_e}}{M^* \int_0^{\xi^*} \frac{e^{-\xi^*/L_e}}{M} d\xi} \quad (47)$$

for $M > 0$.

The function R , on the right hand side of these equations, is defined in Equation (42) and can be expressed in terms of the flame temperature deviation s as

$$R \equiv \frac{r}{s} = \frac{1}{s} \left(\frac{\alpha s + 1}{\alpha + 1} \right)^2 \exp \left[\frac{\varepsilon \alpha}{2} \left(\frac{s - 1}{\alpha s + 1} \right) \right] \quad (48)$$

where nondimensional heat release α and activation energy ε are given by

$$\alpha \equiv \frac{\theta_a - \theta_o}{\theta_o}, \quad \varepsilon \equiv \frac{E_n}{\theta_a} = \frac{E}{R^o T_a} \quad (49)$$

Equations (46) and (47) show that the ratio of the reference mass burning velocity m_o to the local mass flux $|m^*|$ at the reaction sheet is the product of two terms. The first, $1/R$, depends only on the temperature of the reaction sheet while the second term is a function of the reaction sheet location ξ^* as well as L_e and $M(\xi)$.

Measures of Flame Strength

Fuel mass consumption rate per unit flame surface area is an important quantity to characterize the burning rate of the flame. Integration of Equation (16) through the reaction sheet yields

$$\int_{-}^{+} (-w_F) dx = |m^*| \left[\frac{dY_F}{d\xi} \right]_{-}^{+} \quad (50)$$

As will be shown later, the right hand term becomes $m_o Y_{F,o}$ for the normal adiabatic flame, which is not subject to strain. Then the mass consumption rate divided by that of the normal adiabatic flame is given by

$$\frac{\int_{-}^{+} (-w_F) dx}{\left[\int_{-}^{+} (-w_F) dx \right]_{normal}} = \frac{|m^*|}{m_o} \frac{1}{Y_{F,o}} \left| \frac{dY_F}{d\xi} \right|^* \quad (51)$$

where $|dY_F/d\xi|^*$ represents magnitude of the gradients at the reaction sheet as given by Equations (23) and (29). This rate ratio corresponds to the consumption speed ratio used by several authors (Bray and Peters 1994, Poinso *et al.* 1996). When use is made of Equations (40), (35), (46) and (47), Equation (51) becomes

$$\frac{\int_{-}^{+} (-w_F) dx}{\left[\int_{-}^{+} (-w_F) dx \right]_{normal}} = r \quad (52)$$

showing that the consumption rate ratio is equal to the function r defined in Equation (42). It should be noticed that the consumption rate ratio depends only on the flame temperature and is equal to unity at the adiabatic flame temperature, so that the mass burning rate is then equal to the burning rate of the normal flame. This is a natural consequence of the present analysis, in which all reactants are assumed to be consumed at the reaction sheet. From Equations (44) and (45) the consumption rate ratio is always equal to unity when $Le = 1$. We shall see later that the consumption rate ratio is also closely related to the temperature gradient at the reaction sheet.

Another measure of flame strength is the local mass flux ratio $|m^*|/m_o$, which corresponds to the displacement speed ratio used by some authors (Bray and Peters 1994, Bradley *et al.* 1996). It may be evaluated in terms of $M(\xi)$ from Equation (46) or (47). However, unlike the consumption speed ratio, the displacement speed ratio does not automatically reach a value of unity at the adiabatic flame temperature.

Gradients at Reaction Surface (Sheet)

The matching conditions (40) and (43) reveal the significance of the temperature and concentration gradients at the reaction sheet. Using the definitions of θ_a and s , the first matching condition, Equation (43) can be written in the form

$$s = \frac{\frac{-1}{L_e Y_{F,o}} \left(\frac{dY_F}{d\xi} \right)^*}{\frac{1}{(\theta^* - \theta_o)} \left(\frac{d\theta}{d\xi} \right)^*} \quad (53)$$

where the minus sign arises because the $(dY_F/d\xi)^*$ and $(d\theta/d\xi)^*$ always have opposite signs. Equation (53) shows that the deviation, s , of the flame temperature from the adiabatic flame temperature is determined by the supply rate of fuel to the reaction sheet divided by the heat loss rate to the unburned mixture. If $Le = 1$, then these two rates are equal, so $s = 1$ and $\theta^* = \theta_a$. The heat released in the narrow reaction zone produces the temperature gradient in the preheat zone at the reaction sheet. This gradient causes the heat flow which is used to heat the unburned mixture to the flame temperature. In general, if $Le \neq 1$, the flame temperature can be different from the adiabatic value and depends on the mass flow distribution in the preheat zone as can be seen from

Equations (44) and (45). Equation (43) also shows that the heat release rate is controlled through the supply rate of fuel to the reaction sheet by molecular diffusion. At the same time the heat release rate is proportional to the reaction rate in the reaction zone. The second matching condition, Equation (40), leads to the conclusion that the reaction rate is uniquely related to reaction zone temperature as shown by Equation (52). In this way, we see that on the one hand the temperature gradient at the reaction sheet represents the heat release rate while, on the other hand, it also represents the heat required to heat the unburned mixture, as can be seen from the following explanation.

When the energy equation of the outer solution, Equation (17) with no reactive term, is integrated from the unburned mixture to the reaction sheet, we have

$$L_e \left\{ M \frac{d\theta}{d\xi} \right\}^* = \int_{\theta_o}^{\theta^*} |M| d\theta \quad (54)$$

for $M < 0$, and

$$L_e \left\{ M \frac{d\theta}{d\xi} \right\}^* - L_e \left\{ M \frac{d\theta}{d\xi} \right\}_o = \int_{\theta_o}^{\theta^*} |M| d\theta \quad (55)$$

for $M > 0$. These equations suggest that the heat released at the reaction sheet minus any heat lost to the boundary at $\xi = 0$ (there are no heat losses at infinity) is used to heat the mixture to the flame temperature. When $|M| = M_c (> 0)$ is constant, this is just equal to $M_c (\theta^* - \theta_o)$ and is proportional to the constant mass flow rate. When $M \neq \text{constant}$, however, it depends on the change in the mass flow rate in the preheat zone. Therefore, we see that in general the energy required to heat up the unburned mixture is not proportional to the local mass flow, but contains all effects of changes in the mass flow in the preheat zone all the way from the unburned mixture to the sheet.

We introduce the temperature gradient, $p^* = (d\theta/dx)^*$, in the original physical plane at the reaction sheet. This is

$$p^* = \left(\frac{M}{\rho D x^j} \right)^* \left(\frac{d\theta}{d\xi} \right)^* \quad (56)$$

where use has been made of Equation (12). When use is made of Equation (40), the gradient is reduced to

$$p^* = \pm r \frac{\theta_a - \theta_o}{\delta} \quad (M \gtrless 0) \quad (57)$$

where the preheat zone thickness of a normal adiabatic flame is $\delta = \rho\sigma/m_o = \sigma/S_u$ and S_u is the laminar burning velocity of the normal adiabatic flame relative to unburned reactants. Noting that $r = 1$ for such a flame we see that its temperature gradient is $p_o = (\theta_a - \theta_o)/\delta$ so Equation (57) can finally be written

$$p^* = \pm r p_o \quad (M \gtrless 0) \quad (58)$$

This expression shows that p^* is a function of θ^* alone; it becomes equal to p_o whenever θ^* becomes equal to the adiabatic flame temperature θ_a . It also allows the consumption speed ratio to be calculated from $r = |p^*|/p_o$. For these reasons the evaluation of p^* is emphasized in the following examples.

3. Conserved Mass Flow

If the mass flow rate function $M(\xi)$ is specified together with appropriate parameters of the mixture properties, the equations presented above can in principle be solved by numerical or analytical means to determine the flame position ξ^* , its temperature θ^* and the mass consumption rate ratio r . In the following the above results will be applied to some simple flow fields, so as to study the relation between these flame properties, the flow and the properties of unburned gas mixture. The simplest case is when the total mass flow rate function is conserved along the space coordinate, that is $M = M_c = \text{constant}$.

Flames for which $M_c < 0$

Here the detailed geometry of the product sink at $\xi = 0$ is unimportant and we may set $x_{min} = 0$ in Equation (12). For this case Equation (44) gives simply $s = 1$ or $\theta^* = \theta_a$. There is no heat loss to a boundary and the flame temperature is always the adiabatic flame temperature independently of j and Le . Then the mass consumption rate ratio $r = 1$ and $p^* = -p_o$ from Equation (58). Also Equation (46) reveals that magnitude of the mass flux $|m^*|$ becomes equal to m_o , independently of j and Le , and of the flame position. This corresponds to the case of the normal adiabatic flame, and m_o is the mass burning velocity of the normal adiabatic plane flame as derived in classical flame theory (Williams 1985). It is uniquely determined by the kinetic, thermodynamic and transport properties of the unburned mixture. Note that the burning velocity is common to the plane and cylindrical flames, and is therefore unaffected by convex flame curvature. In the cylindrical flame, however, it is not m but $|M_c|$ which is kept constant. Then, from Equation (6) with $j = 1$, the flame location is

$$x^* = |M_c| / m_o \quad (59)$$

showing that the flame position is determined by the value of $|M_c|$.

Flames for which $M_c > 0$

Here we must place an injector at $\xi = 0$ to supply the reactant mass flow

$$m_c = M_c / x_{min}^j$$

where x_{min} is the linear position of the injector ($j = 0$) or the injector radius ($j = 1$). In either case the $\xi = 0$ boundary condition is imposed at $x = x_{min}$. The *planar flame* case $j = 0$ is considered first.

Equation (45) gives

$$s = \frac{1 - e^{-\xi^*/Le}}{1 - e^{-\xi^*}} \quad (60)$$

A deviation of flame temperature occurs when $Le \neq 1$, positive for $Le < 1$ and negative for $Le > 1$, even though there is no strain in the flow. The deviation depends on the flame position. This is because the heat release rate at the reaction sheet is controlled by the diffusion rate of fuel to the sheet on one hand, while the flame temperature depends on the heat loss rate to the injector surface on the other. Both of these rates depend on the flame sheet position, and cancel out when $Le = 1$. The maximum deviation is $s = 1/Le$ for $\xi^* \rightarrow 0$, and it becomes zero as $\xi^* \rightarrow \infty$, suggesting that the deviation is produced when the thickness of the preheat zone is limited. The preheat zone solution Equations (30) and (56) can be manipulated to give the required result

$$p^* = \frac{s(\theta_a - \theta_o)M_c}{(1 - e^{-\xi^*/L_e})\rho\sigma} \quad (61)$$

where M_c is constant, showing that the gradient depends upon the flame location ξ^* . On the other hand, Equation (58) provides an alternative expression for p^* in terms of the properties of the thin reaction zone. Equating these expressions we find

$$\frac{M_c}{m_o} = R \left[1 - \exp\left(-\frac{\xi^*}{L_e}\right) \right] \quad (62)$$

Equation (62) may be solved, together with Equations (48) and (60), to determine the flame position ξ^* . This procedure may be illustrated by considering the special case $L_e = l$ for which $s = R = l$. Then Equation (62) gives

$$\xi^* = \ln \left[\frac{1}{1 - M_c / m_o} \right] \quad (63)$$

Using $\delta = \rho\sigma/m_o$ this may be written

$$\frac{x^*}{\delta} = \frac{m_o}{M_c} \ln \left[\frac{1}{1 - M_c / m_o} \right] \quad (64)$$

which shows that, even in this simple planar flame case, the upstream boundary condition influences the flame position for given mass flux M_c .

The *cylindrical flame* ($Mc > 0, j = 1$) is most easily described in physical space but the dimensionless variable may be recovered from

$$\xi = \frac{M_c L_e}{\delta m_o} \ln \left(\frac{x}{x_{\min}} \right) \quad (65)$$

Equation (45) with $M = \text{constant}$ leads to Equation (60) as before and Equation (65) then enables s to be expressed in terms of x^* . The result is

$$s = \frac{1 - (x_{\min} / x^*)^c}{1 - (x_{\min} / x^*)^{cL_e}} \quad (66)$$

where $c \equiv M_c / (m_o \delta)$. The preheat zone solution leads to

$$p^* = \frac{M_c s(\theta_a - \theta_o)}{m_o \delta x^* \left[1 - (x_{\min} / x^*)^c \right]} \quad (67)$$

which again depends on the flame position. If this is equated to Equation (58), which is the thin reaction zone expression for p^* , the result is an equation for the flame position x^* . This equation together with Equation (66) can be used to calculate x^* and p^* , and other flame properties then follow.

A special case arises if the radius x_{\min} of the mass source at the origin is small so that $x_{\min}/x^* \ll 1$. Then Equation (66) shows that $s \rightarrow 1$ and heat loss to the source is negligible. Equation (67) becomes

$$\frac{p^*}{p_o} = \frac{M_c}{m_o x^*} \quad (68)$$

but Equation (58) shows that with $s = 1$ and hence $r = 1$ we must have $p^* = p_o$. Hence x^* is determined from

$$\frac{x^*}{\delta} = \frac{M_c}{\delta m_o} = \frac{M_c}{\rho \sigma} \quad (69)$$

This result which is equivalent to Equation (59) shows that the sign of the curvature and the direction of the flow are not important provided there is no heat loss.

The following section is concerned with flames in nonuniform flows in circumstances where the constant density assumption significantly simplifies the analysis.

4. Nonuniform Flow

Flames for which $M < 0$

The simplest situation is that where the mass flux decreases linearly towards the origin of the space coordinate, as shown schematically in Figure 3. The mass flow function and mass flux are given by

$$M = -\rho a x^{(j+1)}, \quad m = -\rho a x^j \quad (70)$$

where a is the velocity gradient. The nondimensional coordinate defined in Equation (12) with $x_{min} = 0$ is

$$\xi = ax^2 / 2D \quad (71)$$

and the mass flow rate can be expressed in terms of ξ as

$$M = -\rho\sqrt{2aD\xi} \quad (j=0), \quad M = -2\rho D\xi \quad (j=1) \quad (72)$$

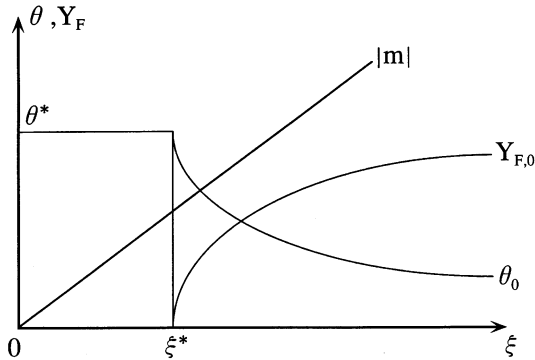


Fig. 3 Schematic representation of mass flux, temperature and fuel concentration distributions for $M < 0$. The flow is from right to left.

The solutions for plane and cylindrical flames will be presented together. Substitution of Equation (72) into Equation (44) yields

$$s = \frac{1}{\sqrt{L_e}} \frac{F_j(\xi^*)}{F_j(\xi^*/L_e)} \tag{73}$$

where $F_o(\xi^*)$ and $F_l(\xi^*)$ are given by

$$F_o(\xi^*) = \frac{e^{-\xi^*}}{\sqrt{\pi} \operatorname{erfc}(\sqrt{\xi^*})}, F_l(\xi^*) = \frac{e^{-\xi^*}}{\sqrt{\xi^*} E(\xi^*)} \tag{74}$$

which are defined in terms of standard functions

$$\operatorname{erfc}(z) = \frac{2}{\sqrt{\pi}} \int_z^\infty e^{-t^2} dt, \quad E(z) = \int_z^\infty \frac{e^{-t}}{t} dt \tag{75}$$

The function $F_l(\xi^*)$ is identical with a function $F(\xi^*)$ introduced in a previous study (Takeno *et al.* 1986b); $F_o(\xi^*)$ and $F_l(\xi^*)$ are shown in Figure 4. It may be seen that F_o is a monotonic function of ξ^* while F_l has a minimum value of $F_c = 1.49144$ at $\xi_c = 0.258951$. When the temperature gradient at the reaction sheet is evaluated, we find

$$p^* = -\sqrt{\frac{2a}{\sigma L_e}} (\theta_a - \theta_o) F_l(\xi^*) \tag{76}$$

It may be seen that for a given value of the velocity gradient, the gradient p^* is proportional to $F_l(\xi^*)$. Figure 4 shows that, in the plane flame, the gradient increases monotonically with the flame location. This is because the mass flow M increases with distance from the origin and, as the

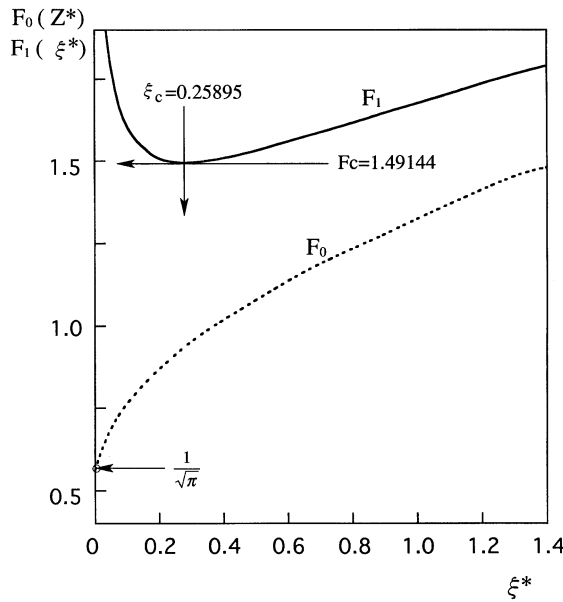


Fig. 4 The functions $F_o(\xi^*)$ and $F_l(\xi^*)$.

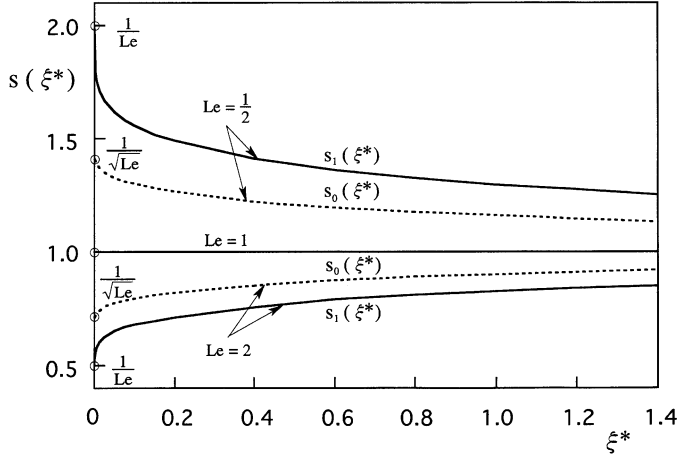


Fig. 5 Influence of Lewis number on flame temperature function $s(\xi^*)$ when $M < 0$.
For planar flames $s = s_0$ and for cylindrical flames $s = s_1$.

flame moves upstream, the amount of heat required to heat the unburned mixture is increased. On the other hand, the gradient becomes smaller as the flame moves downstream and takes a minimum value at zero. At this flame position we still need a finite amount of heat to heat the mixture. In the cylindrical flame, on the other hand, the gradient is always larger than that of the plane flame. It increases as the flame moves upstream in the same way as in the plane flame. What makes a difference is the behavior in the vicinity of the origin. As the flame moves downstream below ξ_c the gradient starts to increase. This is due to the heat divergence effect of the cylindrical flame. In order to supply a finite amount of heat to the mixture, the gradient has to increase without limit as the flame approaches the origin and the flame surface area approaches zero.

The flame temperature depends on the flame position when $Le \neq 1$, and the dependence of the deviation s on ξ^* , calculated from Equation (73) is shown in Figure 5 for representative values of $Le = 2, 1, 1/2$. When Equation (72) is substituted into Equation (46) we have

$$\left| \frac{m^*}{m_o} \right| = \frac{r\sqrt{\xi^*/L_e}}{sF_j(\xi^*/L_e)} = R \frac{\sqrt{\xi^*/L_e}}{F_j(\xi^*/L_e)} \quad (77)$$

Now Equation (77), combined with Equation (73), will determine the flame temperature and position for a given set of values of velocity gradient and unburned gas properties. Equation (77) can be rewritten in the following form.

$$\frac{m_o R}{\rho\sqrt{2a\sigma}} = F_j(\xi^*/L_e) \quad (78)$$

Equation (78) and Figure 4 reveal how the flame position changes with the velocity gradient. As the velocity gradient is increased the left hand side of Equation (78) decreases, and the plane flame approaches the origin without limit reaching the origin at a certain finite value of a . Further increase in a causes extinction at the origin. On the contrary, although the cylindrical flame initially approaches the origin with increasing velocity gradient, at a critical value the flame reaches the critical position below which there are no combustion solutions. Then extinction occurs while the flame is located at a finite distance from the origin. As is explained above, this is due to the combined effect of the decreased mass flux towards the origin and heat divergence in the cylindrical flame.

Flames for which $M > 0$

Here the upstream boundary conditions are given at $\xi = 0$, and this can produce some difficulty in choosing the flow field. We shall study only a relatively simple case where the mass flow function is given by

$$M = \rho b/x \tag{79}$$

where b is a constant to characterize the flow field. A hypothetical reactant mass source is placed at $x = 0$. In the following we present the solutions separately for plane and cylindrical flames, as functions of the original space coordinate x .

Plane Flame ($j = 0$)

The mass flux $m = M$, and the solutions for $b > 0$, that satisfy the appropriate boundary conditions, are given as

$$Y_F = Y_{F,o} \left[1 - \left(\frac{x}{x^*} \right)^{\left(\frac{b}{\sigma} + 1 \right)} \right], \quad \theta = \theta_o + (\theta^* - \theta_o) \left(\frac{x}{x^*} \right)^{\left(\frac{b}{\sigma} + 1 \right)} \tag{80}$$

These solutions show that the concentration and temperature gradients must vanish at $x = 0$, where the mass flux becomes infinitely large. The temperature gradient at the reaction sheet is given by

$$p^* = \left(\frac{1}{L_e} + \frac{b}{\sigma} \right) \frac{(\theta_a - \theta_o)}{x^*} \tag{81}$$

which shows that the gradient decreases monotonically as the flame moves down stream. The first matching condition, given by Equation (43), may be written in terms of the space coordinate x , and substitution of these solutions into it gives the flame temperature deviation as

$$s = \frac{1/L_e + b/\sigma}{1 + b/\sigma} \tag{82}$$

Note that the deviation s is independent of the flame position and is a function of Le and b/σ alone. Substitution of Equation (79) into Equation (40), written in terms of the space coordinate x , gives

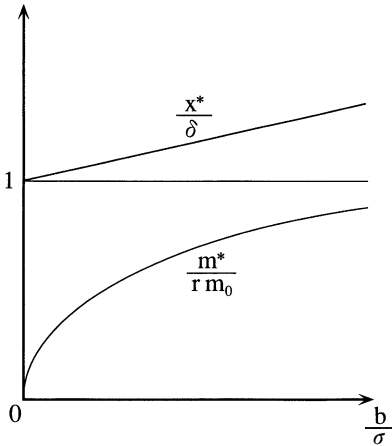


Fig. 6 Flame location x^*/δ and mass flux m^*/m_0 vs b/σ for planar flames with $M > 0$.

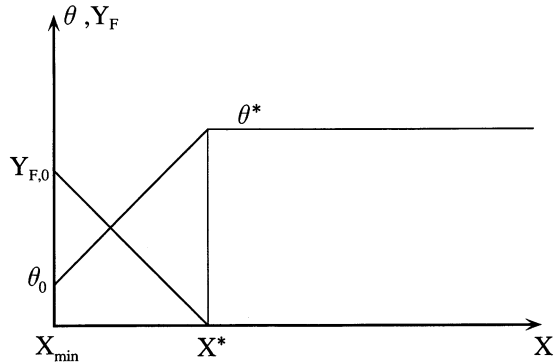


Fig. 7 Temperature and fuel concentration distributions for planar flame with $M > 0$ in the limit $b \rightarrow 0$.

the nondimensional flame position and mass flux as

$$\frac{x^*}{\delta} = R \left(1 + \frac{b}{\sigma} \right), \quad \frac{m^*}{m_o} = \frac{R}{1 + \sigma/b} \quad (83)$$

Since $R = R(s)$ they are determined as functions of L_e and b/σ alone and their dependence are shown in Figure 6. As b/σ is increased, the flame position moves downstream and the normalized mass flux increases gradually to reach unity at an infinitely large value of b/σ . On the contrary, the limit $b \rightarrow 0$ corresponds to a case with no convective flow. In this limit the gradients become independent of position, and we have a flame supported by molecular diffusion alone; its structure is shown schematically in Figure 7. The flame temperature deviation becomes equal to $1/L_e$.

Cylindrical Flame ($j = 1$)

The flow field is similar to that studied in an axisymmetric tubular flame, in which the unburned mixture is injected outward from the line source on the axis (Takeno *et al.* 1994, Zhu *et al.* 1995a, 1995b). The mass flux becomes

$$m = \rho b/x^2 \quad (84)$$

There are no solutions for $b = 0$ that satisfy the boundary conditions, and we are concerned only with the case where $b > 0$. The solutions are given by

$$Y_F = Y_{F,o} - Y_{F,o} \frac{E(t)}{E(t^*)}, \quad \theta = \theta_o + (\theta^* - \theta_o) \frac{E(t/L_e)}{E(t^*/L_e)} \quad (85)$$

where $t = b/Dx$. We notice, here again, that the gradients become zero at $x = 0$. The temperature gradient at the flame surface is given by

$$p^* = \frac{D}{bL_e} (\theta_a - \theta_o) \frac{t^* e^{-t^*}}{E(t^*)} \quad (86)$$

The gradient again decreases monotonically as the flame moves downstream. Now substitution of the solutions into the matching conditions gives the flame temperature derivation and the normalized mass flux as

$$s = \frac{1}{L_e} \frac{e^{t^*/L_e} E(t^*/L_e)}{e^{t^*} E(t^*)} \quad (87)$$

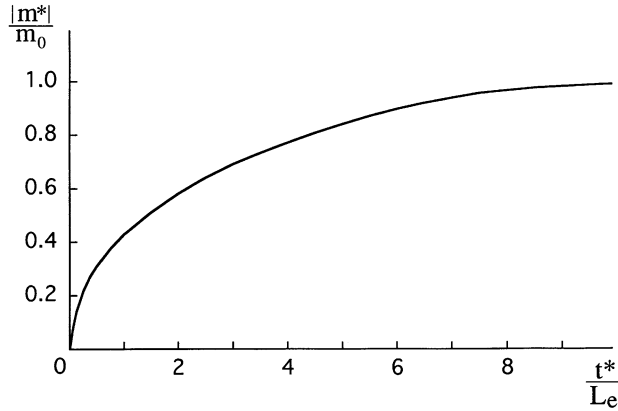


Fig. 8 Cylindrical flame with $M > 0$: mass flux ratio $|m^*|/m_o$.

$$\frac{m^*}{m_o} = R \left(\frac{t^*}{L_e} \right) e^{t^*/L_e} E(t^*/L_e) \quad (88)$$

which determine the flame position for a given set of values of b and mixture properties. The term on the right hand side of Equation (88) is plotted schematically against t^*/L_e in Figure 8. As is seen in the figure, the local mass flux increases as t^*/L_e increases, or as the flame moves upstream towards the axial line source.

5. Effects of Flames Stretch

In nonuniform or unsteady flows the flame is subjected to stretch (Chung and Law 1988, Candel and Poinso 1990) due to tangential strain in the plane of the flame together with propagation in the presence of flame curvature. In the present analysis the flame stretch $1/\tau_s$ is given as

$$\frac{1}{\tau_s} \equiv \frac{1}{\Delta A} \frac{d\Delta A}{dt} = \left(\frac{\partial v}{\partial y} \right)_{x^*} = - \left(\frac{1}{\rho x^j} \frac{dM}{dx} \right)_{x^*} \quad (89)$$

where ΔA is the area of an element of flame surface and d/dt is a Lagrangian derivative following the flame element. The final equality follows from Equation (8). It should be noticed that the mass flow rate must not increase as the flame is approached from the unburned gas side so the stretch is always positive or zero in this work. The stretch is zero for all the conserved mass flow cases considered here both with and without curvature.

We define a local flame stretch $1/\tau_s^*$ at the flame position $x = x^*$. Then for the nonuniform mass flow cases considered above we have

$$\frac{1}{\tau_s^*} = (j+1)a \quad (M < 0); \quad \frac{1}{\tau_s^*} = \frac{b}{(x^*)^{(j+2)}} \quad (M > 0) \quad (90)$$

Note in Equation (90) τ_s^* depends only on the velocity gradient a when $M < 0$, whereas when $M > 0$ and more generally τ_s^* is influenced both by the velocity gradient and also by the flame location x^* . The reason is as follows. With the sign convention adopted here flames for which $M < 0$ have preheat zones which are not constrained by flow boundaries and which are therefore free to respond to the velocity gradient a . On the other hand when $M > 0$ the preheat zone structure will also be influenced by the boundary condition imposed at $x = 0$ unless $x^* \gg \delta$. The dimensionless stretch K is defined in terms of the characteristic laminar flame time δ/S_u where $\delta = \sigma/S_u$. Then

$$K = \frac{\delta}{S_u \tau_s^*} = \frac{\sigma \rho}{m_o^2 (x^*)^j} \left| \frac{dM}{dx} \right|^* \quad (91)$$

In the four nonuniform mass flow cases the dimensionless flame stretch can be expressed as

$$K = \frac{\sigma \rho^2}{m_o^2} a = \frac{(j+1)}{2} \frac{L_e}{\xi^*} \left(\frac{m^*}{m_o} \right)^2 \quad (M < 0, j = 0, 1) \quad (92)$$

$$K = \frac{\sigma}{b} \left(\frac{m^*}{m_o} \right)^2 \quad (M > 0, j = 0) \quad (93)$$

$$K = \frac{L_e}{t^*} \left(\frac{m^*}{m_o} \right)^2 \quad (M > 0, j = 1) \quad (94)$$

Equations (46) and (47) show that $|m^*|/m_o$ is the product of the function $1/R$, which depends only

on reaction sheet temperature s , and an expression depending on L_e and the reaction sheet location. It follows that K is $1/R^2(s)$ times a function of L_e and the reaction sheet location ξ^* . This analysis of flames in nonuniform flows identifies a convenient and natural independent variable in each of cases studied. In terms of primitive variables, normalized by the local stretch $1/\tau_s^*$ and thermal diffusivity σ these independent variables are

$$\xi = \frac{L_e x^2}{2(j+1)\tau_s \sigma} \quad (M < 0, j = 0, 1) \quad (95)$$

$$\frac{b}{\sigma} = \frac{x^2}{\tau_s \sigma} \quad (M > 0, j = 0); \quad t = \frac{L_e x^2}{\tau_s \sigma} \quad (M > 0, j = 1) \quad (96)$$

In principle, it is now possible to use Equations (92) – (94) together with the solutions derived above in order to express the two measures of flame strength, namely r (see Equation 52) and $|m^*|/m_o$ (See Equations 46 and 47), in terms of K and L_e . Use of Equations (77), (83) and (88) to eliminate the mass flux ratio $|m^*|/m_o$ from Equations (92) – (94) shows that K depends on the flame location, ξ^* , as well as on the flow parameters, in a complicated way. Some simplification can be achieved (Libby *et al.* 1983) in the limit $L_e - 1 \ll 1$ but explicit analytical solutions are still not obtained. Fortunately it is not necessary to perform any algebra in order to see that the resulting expressions for $r(K, L_e)$ and $|m^*(K, L_e)|/m_o$ will not be all the same. That is, these flame strength parameters depend not only on the local flame stretch K and Lewis number L_e but also on the flow geometry as expressed in the mass flux function $M(\xi)$ for the preheat zone. This behavior should be contrasted with the temperature gradient at the reaction surface $p^* = (d\theta/dx)^*$ which takes these geometry effects into account and uniquely determines the consumption speed ratio as $r = |p^*|/p_o$. It follows from this result that r is a unique function of the instantaneous scalar dissipation $\chi_\theta = 2\sigma p^2$ evaluated at the reaction surface. Note that the scalar dissipation χ_θ plays an important role in theories of turbulent combustion (Bray 1996).

We now explore the question of whether or not $r(K, L_e)$ and $|m^*(K, L_e)|/m_o$ continue to be dependent on geometry in the limit of weak stretch.

Dependence on Weak Stretch

As we have seen the dependence of flame properties on the flame stretch K is generally nonlinear and algebraically complicated. In the following we study the limit where $K \ll 1$.

Initially, flames for which $M < 0$ are considered. The Equations (44) and (91) show that $s = 1$ when $M = \text{constant}$ and $K = 0$, so it is appropriate to consider small departures from unity of the flame temperature parameter s . The quantity R is a function of s and from Equation (48)

$$\frac{dR}{ds} = \frac{1}{(\alpha + 1)^2} \left[\left(\alpha^2 - \frac{1}{s^2} \right) + \frac{\varepsilon \alpha (\alpha + 1)}{2s} \right] \exp \left[\frac{\varepsilon \alpha}{2} \left(\frac{s-1}{\alpha s + 1} \right) \right] \quad (97)$$

where the constants α and ε are defined in Equation (49). Then

$$\left(\frac{dR}{ds} \right)_{s=1} = \frac{2\alpha + \varepsilon \alpha - 2}{2(\alpha + 1)} \equiv \gamma \quad (98)$$

where γ is a constant of order unity. It follows that

$$R(s) \approx 1 + \gamma(s-1) + O[(s-1)^2] \quad (99)$$

We must now determine how s varies with K . Equation (92) indicates that $K \rightarrow 0$ as $\xi^* \rightarrow \infty$. A small quantity k is defined as

$$k = \frac{(j+1)L_e}{2\xi^*} \quad (M < 0, j = 0, I) \quad (100)$$

When $\xi^* \rightarrow \infty$ the functions $\operatorname{erfc}(\sqrt{\xi^*})$ and $E(\xi^*)$ may be expanded as power series in $1/\xi^*$. The functions $F_o(\xi^*)$ and $F_I(\xi^*)$ which are defined in Equation (74) may then be written

$$F_o(\xi^*) = \sqrt{\xi^*} \left(1 + \frac{1}{2\xi^*} + O\left(\frac{1}{\xi^{*2}}\right) \right); F_I(\xi^*) = \sqrt{\xi^*} \left(1 + \frac{1}{\xi^*} + O\left(\frac{1}{\xi^{*2}}\right) \right) \quad (101)$$

Substitution in Equation (73) and use of Equation (100) leads to

$$s = 1 + \frac{(1-L_e)}{L_e} k + O(k^2) \quad (j = 0, I) \quad (102)$$

Further substitution into Equation (99) yields

$$R = 1 + \gamma \frac{(1-L_e)}{L_e} k + O(k^2) \quad (j = 0, I) \quad (103)$$

$$r = 1 + \frac{(1+\gamma)(1-L_e)}{L_e} k + O(k^2) \quad (j = 0, I) \quad (104)$$

while Equation (77) may be written

$$\left| \frac{m^*}{m_o} \right| = 1 + \left[\frac{\gamma(1-L_e)}{L_e} - 1 \right] k + O(k^2) \quad (j = 0, I) \quad (105)$$

Finally, the small parameter k must be related to the stretch K . Substituting Equation (105) into Equation (92) we find

$$K = k \left(\frac{m^*}{m_o} \right)^2 = k \left[1 + 2 \left\{ \frac{\gamma(1-L_e)}{L_e} \right\} k + O(k^2) \right] \quad (j = 0, I) \quad (106)$$

To evaluate Equations (104) and (105) to first order we require only $K = k + O(k^2)$. Then with the usual sign convention

$$r = 1 - \mu_r K + O(K^2) \quad (j = 0, I) \quad (107)$$

$$\left| \frac{m^*}{m_o} \right| = 1 - \mu_m K + O(K^2) \quad (j = 0, I) \quad (108)$$

where μ_r and μ_m are Markstein numbers in terms of unburned gas properties which are given by

$$\mu_r = -\frac{(\gamma+1)(1-L_e)}{L_e} = -\frac{\alpha(4+\varepsilon)}{2(\alpha+1)} \frac{(1-L_e)}{L_e} \quad (109)$$

$$\mu_m = 1 - \frac{\gamma(1-L_e)}{L_e} = 1 - \frac{(2\alpha+\varepsilon\alpha-2)}{2(\alpha+1)} \frac{(1-L_e)}{L_e} \quad (110)$$

Clearly, these two expressions are not the same. We have $\mu_r > 0$ for $L_e > 1$ so the consumption speed ratio is decreased by positive stretch if $L_e > 1$ and increased if $L_e < 1$. On the other hand $\mu_m > 0$ when

$$L_e > L \equiv \frac{2 + \varepsilon - 2/\alpha}{4 + \varepsilon} \quad (111)$$

where $L < 1$ for realistic values of ε and α . Consequently, if L_e is in the range $L < L_e < 1$, positive stretch decreases the displacement speed ratio $|m^*|/m_o$ but increases the consumption speed ratio r .

The analysis presented in this paper shows that both μ_r and μ_m include effects of flame stretch on the temperature of the reaction sheet. Since $dr/ds = (1 + \gamma)$, Eq.(104) shows that μ_r describes this effect alone. On the other hand, μ_m is also influenced by the location x^* of the reaction sheet which varies with stretch through the dependence of $|m^*|$ on x^* . A consequence is that, if $L_e = 1$, $\mu_r = 0$, confirming the earlier result that the consumption speed is then independent of stretch. In contrast, $\mu_m(L_e = 1) = 1$ because stretch still influences x^* .

In view of the many simplifications introduced into the present analysis quantitatively accurate predictions of Markstein numbers should not be expected. The Markstein numbers originates in the temperature dependence of the chemical reaction rate and in real flames is strongly influenced by details of the complex reaction mechanism. However, if we assume $\varepsilon \gg 1$ in Equation (110), the Markstein number expression obtained in the constant density analysis of Sivashinsky (1977) is recovered. Numerical analysis (Bradley *et al.* 1996) confirms our prediction $\mu_r \neq \mu_m$. However, for the cases computed (Bradley *et al.* 1996), the relative magnitudes of μ_r and μ_m are not well described by Equations (109) and (110).

Now consider flames for which $M > 0$. For these cases, we define the small parameter k , analogous to Equation (100), to be

$$k = \sigma/b \quad (j = 0); \quad k = L_e/t^* \quad (j = 1) \quad (112)$$

Equations (82) and (87) show that $s \rightarrow 1$ as $k \rightarrow 0$ in both of these cases so Equations (97) and (99) are applicable. Analysis similar to that for $M < 0$ then proves that Equations (107) – (110) are valid for all four cases. We conclude that these expressions are independent of both the configuration of the flow and the curvature of the flame. Note that the stretch K is defined at the flame surface, whose location is initially unknown, while stretch is a function of position in the case where $M > 0$, $j = 0, 1$ (see Equation 90). The flame location in physical space can be found from

$$\frac{\delta}{x^*} = \frac{K}{(j+1)} \left[1 + \mu_m K + O(K^2) \right] \quad (M < 0; j = 0, 1) \quad (113)$$

$$\frac{\delta}{x^*} = K \left[1 + \mu_m K + O(K^2) \right] \quad (M > 0; j = 0, 1) \quad (114)$$

showing that the distance x^* , between the flame and the origin, divided by the unstretched flame preheat zone thickness, δ , varies like $1/K$.

Conclusions

1. A simple analysis is presented of steady, planar and cylindrical laminar flames assuming a large activation energy, constant density and constant transport coefficients. Matched inner and outer solutions predict flame properties in terms of an arbitrary distribution through the preheat zone of the mass flux function M describing the nonuniformity of the flow approaching the reaction zone. Different functions $M(x)$ correspond to different flame and flow geometries. Because the analysis is applicable to any function $M(x)$ it provides a convenient framework for a simple description of laminar flame propagation in nonuniform flows.

2. The analysis is illustrated with simple examples involving both uniform and nonuniform flows approaching the reaction zone. The solutions are shown to depend upon the flame geometry (plane or cylindrical) as well as on the sign and character of $M(x)$. In the nonuniform cases with $M < 0$ important differences are identified between the solutions for planar and cylindrical flames. The planar flame reaches the origin at a finite value of the flame stretch. On the contrary, increasing stretch causes the cylindrical flame to approach a finite critical distance from the origin. At this critical radius the flame is extinguished due to the combined effects of decreased mass flux towards the origin and heat divergence in the preheat zone.
3. The dimensionless stretch parameter K is evaluated for the nonuniform flow cases. The results clearly show that the measures of flame strength, the consumption speed ratio, r , and displacement speed ratio $|m^*|/m_o$, are not unique functions of K ; they depend also on flame and flow geometries. Because K is a local property, evaluated at the reaction surface, it cannot take account of variations in the mass flux function $M(x)$ throughout the preheat zone. In the limit of weak stretch, $K \ll 1$, it is shown that all four nonuniform flow cases reduce to the same linear relationships for $r(K)$ and $|m^*(K)|/m_o$. Separate Markstein numbers, μ_r and μ_m , respectively, are evaluated from these relationships as functions of the Lewis number and other parameters. They are independent of curvature.
4. Irrespective of geometry, the temperature at the reaction surface is shown to result from a balance between heat release due to reaction and heat loss by conduction to the preheat zone. This conduction heat loss is influenced by the flame and flow geometries through $M(x)$. The temperature gradient at the reaction surface, $p^* = (d\theta/dx)^*$, takes these geometry effects into account and uniquely determines the consumption speed ratio as $r = |p^*|/p_o$. No such simple general relationship has been found for the displacement speed ratio which is influenced by the reaction sheet location. It is concluded that p^* rather than K should be adopted as the appropriate parameter for predicting and correlating the propagation of laminar flames in nonuniform flow fields.

Acknowledgment

TT would like to extend his sincere thanks to the Japan Society for the Promotion of Science for the opportunities to spend wonderful days at Cambridge. He would also like to extend his thanks to the YAMAHA MOTOR Foundation for its support in the initial stage of the authors' cooperation.

References

- Bradley, D., Gaskell, P.H. and Gu, X.J.** 1996. Burning velocities, Markstein lengths and flame quenching for spherical methane-air flames; a computational study. *Combust. Flame* **104**,176–198.
- Bray, K.N.C. and Peters, N.** 1994. Laminar flamelets in turbulent flames. In *Turbulent Reacting Flows* (ed. P.A. Libby and F.A. Williams), Academic Press, London.
- Bray, K.N.C.** 1996. The challenge of turbulent combustion. *26th Int. Symp. on Combust.*, The Combustion Institute, Pittsburgh, pp. 1–26.
- Buckmaster, J.D.** 1979. The quenching of a deflagration wave held in front of a bluff body, *17th Int. Symp. on Combust.*, The Combustion Institute, Pittsburgh, pp. 835–842.

- Backmaster, J.D. and Ludford, G.S.S.** 1982. *Theory of Laminar Flames*, Cambridge University Press, Cambridge.
- Buschmann, A., Dinkelacker, F., Schaffer, M. and Wolfrum, J.** 1996. Measurement of the instantaneous detailed flame structure in turbulent premixed combustion, *26th Int. Symp. on Combust.*, The Combustion Institute, Pittsburgh, pp. 437–445.
- Candel, S. and Poinso, T.** 1990. Flame stretch and the balance equation for the flame area. *Combust. Sci. and Tech.*, **70**, 1–15.
- Chen, Y.C., Peters, N., Schneemann, G.A., Wruck, N., Renz, U. and Mansour, M.S.** 1996. The detailed structure of highly stretched turbulent premixed methane-air flames. *Combust. Flame* **107**, 223–244.
- Chung, S.H. and Law, C.K.** 1984. An invariant derivation of flame stretch. *Combust. Flame* **55**, 123–126.
- Chung, S.H. and Law, C.K.** 1988. An integral analysis of the structure and propagation of stretched premixed flames. *Combust. Flame* **72**, 325–336.
- Chung, S.H. and Law, C.K.** 1989. An analysis of some nonlinear premixed flame phenomena. *Combust. Flame* **75**, 309–323.
- Clavin, P. and Williams, F.A.** 1982. Effects of molecular diffusion and thermal expansion on the structure and dynamics of premixed flames in turbulent flows of large scale and low intensity. *J. Fluid Mech.*, **116**, 251.
- Clavin, P. and Joulin G.** 1983. Premixed flames in large scale and high intensity turbulent flow. *J. de Physique Lettre*, **44**, L-1.
- Clavin, P.** 1985. Dynamic behavior of premixed flame fronts in laminar and turbulent flows. *Prog. Energy Combust. Sci. and Tech.*, **11**, 1–59.
- Joulin, G.** 1994. On the response of premixed flames to time-dependent stretch and curvature. *Combust. Sci. and Tech.*, **97**, 219–229.
- Law, C.K.** 1988. Dynamics of stretched flames. *22nd Int. Symp. on Combust.*, The Combustion Institute, Pittsburgh, pp. 1381–1402.
- Libby, P.A. and Williams, F.A.** 1982. Structure of laminar flamelets in premixed turbulent flames. *Combust. Flame* **44**, 287–303.
- Libby, P.A. and Williams, F.A.** 1983. Strained premixed laminar flames under nonadiabatic conditions. *Combust. Sci. and Tech.*, **31**, 1–42.
- Libby, P.A., Linan, A. and Williams, F.A.** 1983b. Strained premixed laminar flames with nonunity Lewis numbers. *Combust. Sci. and Tech.*, **34**, 257–293.
- Libby, P.A. and Williams, F.A.** 1984. Strained premixed laminar flames with two reaction zones. *Combust. Sci. and Tech.*, **37**, 221–252.
- Libby, P.A. and Williams, F.A.** 1984. Premixed laminar flames with general rates of strain. *Combust. Sci. and Tech.*, **54**, 237.
- Libby, P.A., Peters, N. and Williams, F.A.** 1989. Cylindrical premixed flames. *Combust. Flame* **75**, 265–280.
- Linan, A. and Williams, F.A.** 1993. *Fundamental Aspects of Combustion*. Oxford University press.
- Matalon, M. and Matkowsky, B.J.** 1982. Flames as gasdynamic discontinuities. *J. Fluid Mech.* **124**, 239.
- Nishioka, M., Takeno, T. and Ishizuka, S.** 1988. Effects of variable density on a tubular flame. *Combust. Flame* **73**, 287–301.
- Nishioka, M., Inagaki, K., Ishizuka, S. and Takeno, T.** 1991. Effects of pressure on structure and extinction of tubular flame. *Combust. Flame* **86**, 90–100.
- Nishioka, M., Nakagawa, S., Ishikawa, Y. and Takeno, T.** 1994. NO emission characteristics of methane-air double flame. *Combust. Flame* **98**, 127–138.
- O’Young, F. and Bilger, R.W.** 1997. Scalar gradient and related quantities in turbulent premixed flames. *Combust. Flame* **98**, 682–700.
- Peters, N.** 1986. Laminar flamelet concepts in turbulent combustion. *21st Int. Symp. on Combust.*, The Combustion Institute, Pittsburgh, pp. 1231–1250.
- Peters, N. and Williams, F.A.** 1987. The asymptotic structure of stoichiometric methane-air flames. *Combust. Flame* **68**, 185–207.
- Peters, N. and Rogg, B.** Eds. 1993. *Reduced kinetic mechanisms for applications in combustion systems*. Springer Verlag, Berlin.
- Poinso, T., Echekki, T. and Mungal, M.S.** 1992. A study of the laminar flame tip and implications for

premixed turbulent combustion. *Combust. Sci. and Tech.*, **81**, 45–73.

- Poinsot, T., Veynante, D. and Candel, S.** 1991. Quenching processes and premixed turbulent combustion diagrams. *J. Fluid Mech.* **228**, 562–605.
- Poinsot, T., Candel, S. and Trounev, A.** 1995. Applications of direct numerical simulation to premixed turbulent combustion. *Prog. Energy Combust. Sci.* **21**, 531–576.
- Sivashinsky, G.I.** 1977. Nonlinear analysis of hydrodynamics instability in laminar flames; I: Derivation of basic equations. *Acta Astronautica* **4**, 1117–1206.
- Takeno, T. and Ishizuka, S.** 1986a. A tubular flame theory. *Combust. Flame* **64**, 83–98.
- Takeno, T., Nishioka, M. and Ishizuka, S.** 1986b. A theoretical study of extinction of a tubular flame. *Combust. Flame* **66**, 271–283.
- Takeno, T. and Nishioka, M.** 1993. Species conservation and emission indices for flames described by similarity solutions. *Combust. Flame* **92**, 465–468.
- Takeno, T., Zhu, X.L. and Nishioka, M.** 1994. Theoretical studies on stability of a tubular flame (in Japanese). *Combust. Research* **97**, 47–59.
- Williams, F.A.** 1985. *Combustion Theory*, 2nd Ed. Benjamin/Cummings, Menlo Park, California.
- Zhu, X.L., Nishioka M., Tamura, M., Nakamura, Y. and Takeno, T.** 1995a. Effects of detailed kinetics and heat loss on a tubular flame (in Japanese). *Combust. Research* **99**, 43–56.
- Zhu, X.L., Nishioka M., Tamura, M., Nakamura, Y. and Takeno, T.** 1995b. NO emission characteristics of tubular flame (in Japanese). *Combust. Research* **100**, 45–61.